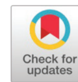

Residual stress measurement of {112}-oriented CrN layers in CrN/Cr multilayer films

Kazuya Kusaka,[1,a)] Kenta Shirasaka,[2] Daisuke Yonekura,[1] and Yuta Tanaka[3]
[1]*Institute of Technology and Science, Tokushima University, 2-1, Minamijosanjima, Tokushima, Tokushima 7708506, Japan*
[2]*Graduate School of Advanced Technology and Science, Tokushima University, 2-1, Minamijosanjima, Tokushima, Tokushima 7708506, Japan*
[3]*Materials Department, Research Laboratory, IHI Corporation, 1, Shin-nakahara-cho, Isogo-ku, Yokohama, Kanagawa 235-8501, Japan*

(Received 3 July 2019; accepted 16 October 2019; published 31 October 2019)

In this work, the authors propose and verify a method of measuring the residual stress of {112}-oriented chromium nitride (CrN) layers in CrN/Cr multilayer thin films. The CrN layers of a CrN/Cr multilayer film deposited on a Ti6Al4V substrate by arc ion plating form both a randomly oriented mixed crystal structure and a {112}-oriented structure. Therefore, accurate stress measurement of the CrN layers cannot be performed by applying the $\sin^2\psi$ x-ray method assuming an isotropic homogeneous material. To overcome this obstacle, the proposed method to measure the residual stress uses four CrN-422 diffractions: at $\psi = 0°$, 33.56°, 48.19°, and 60.00°. Next, the authors vary the density of Cr droplets on the film surface to evaluate how it affects the residual stress in the CrN/Cr multilayer film. The results indicate that the Cr layer has a residual compressive stress of −350 to −530 MPa and that the two CrN layers have a very large residual compressive stress of −3.5 to −8.2 GPa. In addition, both residual compressive stresses decrease with increasing droplet density. *Published by the AVS.* https://doi.org/10.1116/1.5118682

I. INTRODUCTION

Chromium nitride (CrN) films prepared by physical vapor deposition and chemical vapor deposition have greater heat resistance than films deposited by electroplating. In addition, because these films are very hard and have desirable sliding characteristics, they are used not only for coating cutting tools[1] and die-castings[2] but also for coating piston rings and connecting rods in automobile engines.[3,4]

Multilayering is very useful to improve the fatigue strength of coatings because multilayer coatings suppress crack propagation thanks to ductile spacing layers of appropriate thickness.[5,6] In the present study, we deposit CrN/Cr multilayer films on titanium alloy substrates to augment the antierosion effect.

These multilayer films develop residual stress because of the different atomic spacing, coefficients of thermal expansion, temperature, and cooling conditions between the film and substrate. Significant residual stress may cause microcracks in the film or cause the film to peel away from the substrate. In addition, a film deposited by arc ion plating has the problem that numerous droplets adhere to the film.[7–9] Because these droplets can be at the origin of film damage, the relationship between droplet density and residual stress needs to be well understood. In recent years, many researchers have been working on the residual stress of thin films.[10,11]

The characterization of CrN/Cr multilayer films deposited on the titanium alloy substrate that is the subject of this study has been reported by Wieciński *et al.*[5,12–14] In this study, we measure the residual stress in the Cr and CrN layers of CrN/Cr multilayer films deposited on the titanium alloy substrates. Because the CrN layers form both a randomly oriented mixed crystal structure and a {112}-oriented structure, the stress cannot be measured by using the $\sin^2\psi$ x-ray method.[15] Although Tanaka *et al.*[16] and Ejiri *et al.*[17] have proposed x-ray methods to measure the stress of cubic polycrystalline thin films with {111}, {001}, and {110} fiber textures, no analogous technique to measure the stress in a {112}-oriented film has yet been reported. To rectify this situation, we propose and verify herein an x-ray method to measure the residual stress of {112}-oriented CrN layers in CrN/Cr multilayer thin films. In addition, we investigate how the surface density of Cr droplets affects the residual stress in CrN/Cr multilayer films.

II. THEORY

X-ray analytical techniques may be used to measure the strain in a crystal lattice. In such methods, the strain is expressed in the laboratory coordinate system L_i, and the stress expressed in the specimen coordinate system S_i is calculated by using the elastic constant expressed in the crystal coordinate system X_i. Furthermore, the transformed crystal coordinate system X'_i is defined, where the X'_3 axis is the [112] axis. Figure 1 shows the relationship between these four coordinate systems. Next, the transformation matrices between the four coordinate axes are defined to permit the transformations depicted in Fig. 2. The transformation matrix α_{ij} from

Note: This paper is part of the Conference Collection: 15th International Symposium on Sputtering and Plasma Processes (ISSP2019).
[a)]Electronic mail: kusaka@tokushima-u.ac.jp

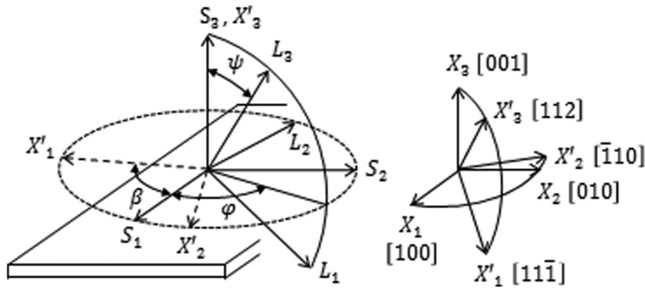

FIG. 1. Relationship between the four coordinate systems L_i, S_i, X'_i, and X_i.

X'_i to X_i is

$$\underline{\alpha} = (\alpha_{ij}) = \begin{pmatrix} \frac{1}{\sqrt{3}} & \frac{1}{\sqrt{3}} & -\frac{1}{\sqrt{3}} \\ -\frac{1}{\sqrt{2}} & \frac{1}{\sqrt{2}} & 0 \\ \frac{1}{\sqrt{6}} & \frac{1}{\sqrt{6}} & \frac{2}{\sqrt{6}} \end{pmatrix}. \quad (1)$$

The transformation matrices ω_{ij}, β_{ij}, π_{ij}, and γ_{ij} are

$$\underline{\omega} = (\omega_{ij}) = \begin{pmatrix} \cos\psi\cos\varphi & \cos\psi\sin\varphi & -\sin\psi \\ -\sin\varphi & \cos\varphi & 0 \\ \sin\psi\cos\varphi & \sin\psi\sin\varphi & \cos\psi \end{pmatrix}, \quad (2)$$

$$\underline{\beta} = (\beta_{ij}) = \begin{pmatrix} \cos\beta & \sin\beta & 0 \\ -\sin\beta & \cos\beta & 0 \\ 0 & 0 & 1 \end{pmatrix}, \quad (3)$$

$$\underline{\pi} = \underline{\beta} \times \underline{\alpha}, \quad (4)$$

$$\underline{\gamma} = \underline{\omega} \times \underline{\pi}. \quad (5)$$

We then use the following relational expression between the elastic compliance s'_{ijkl} represented in the X'_i system and the elastic compliance s_{pqrs} represented in the X_i system to obtain

$$s'_{ijkl} = \alpha_{ip}\alpha_{jq}\alpha_{kr}\alpha_{ls}s_{pqrs}. \quad (6)$$

Next, we expand Eq. (6), substitute Eq. (1), and use the correspondence between the tensor representation s'_{ijkl} and the matrix representation s'_{ij} of the elastic compliance of the crystal to obtain[18]

$$s'_{ij} = \begin{pmatrix} s'_{11} & s'_{12} & s'_{12} & s'_{14} & 0 & 0 \\ s'_{12} & s'_{22} & s'_{23} & s'_{24} & s'_{25} & s'_{26} \\ s'_{12} & s'_{23} & s'_{22} & s'_{24} & -s'_{25} & -s'_{26} \\ s'_{14} & s'_{24} & s'_{24} & s'_{44} & s'_{26} & s'_{25} \\ 0 & s'_{25} & -s'_{25} & s'_{26} & s'_{55} & -s'_{14} \\ 0 & s'_{26} & -s'_{26} & s'_{25} & -s'_{14} & s'_{55} \end{pmatrix}, \quad (7)$$

where each matrix component s'_{ij} is related to the cubic elastic compliances s_{11}, s_{12}, and s_{44} as follows:

$$\begin{aligned} s'_{11} &= \frac{1}{3}s_{11} + \frac{2}{3}s_{12} + \frac{1}{3}s_{44}, \\ s'_{12} &= \frac{1}{3}s_{11} + \frac{2}{3}s_{12} - \frac{1}{6}s_{44}, \\ s'_{14} &= -\frac{\sqrt{3}}{6}s_{44}, \\ s'_{22} &= \frac{1}{2}s_{11} + \frac{1}{2}s_{12} + \frac{1}{4}s_{44}, \\ s'_{23} &= \frac{1}{6}s_{11} + \frac{5}{6}s_{12} - \frac{1}{12}s_{44}, \\ s'_{24} &= \frac{\sqrt{3}}{12}s_{44}, \\ s'_{25} &= \frac{\sqrt{2}}{6}s_{11} - \frac{\sqrt{2}}{6}s_{12} - \frac{\sqrt{2}}{12}s_{44}, \\ s'_{26} &= -\frac{\sqrt{6}}{12}s_{44}. \end{aligned} \quad (8)$$

X rays may be used to measure the crystal lattice strain ε^L_{33} in the L_3 direction, whereas the stress σ^S_{ij} to be determined is expressed in the sample coordinate system. If the stress tensor and the strain tensor in the S_i system, X'_i system, and L_i system are expressed as $(\sigma^S_{ij}, \varepsilon^S_{ij})$, $(\sigma^{X'}_{ij}, \varepsilon^{X'}_{ij})$, and $(\sigma^L_{ij}, \varepsilon^L_{ij})$, the following relationships hold:

$$\begin{aligned} \varepsilon^L_{33} &= \gamma_{3i}\gamma_{3j}\varepsilon^{X'}_{ij}, \\ \varepsilon^{X'}_{ij} &= s'_{ijkl}\sigma^{X'}_{kl}, \\ \sigma^{X'}_{kl} &= \pi_{kp}\pi_{lq}\sigma^S_{pq}. \end{aligned} \quad (9)$$

Therefore, the relation between the strain ε^L_{33} measured by x rays and the stress σ^S_{ij} to be determined is

$$\varepsilon^L_{33} = \gamma_{3i}\gamma_{3j}s'_{ijkl}\pi_{kp}\pi_{lq}\sigma^S_{pq}. \quad (10)$$

Furthermore, if the residual stress is equi-biaxial, then we may use

$$\varepsilon^L_{33} = \frac{1}{6}s_{44}\sigma\sin^2\psi + \frac{1}{3}(2s_{11} + 4s_{12} - s_{44})\sigma. \quad (11)$$

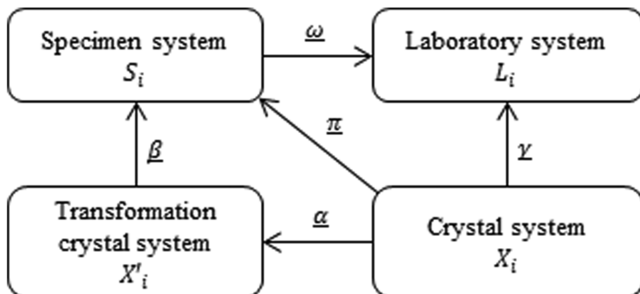

FIG. 2. Definition of transformation matrices.

Therefore, the stress is given by

$$\sigma = \frac{6}{s_{44}} \frac{\partial \varepsilon_{33}^{L}}{\partial \sin^2 \psi}. \tag{12}$$

Next, by converting the relationship between stress and strain expressed by Eq. (12) into a relationship between stress and diffraction angle, we obtain

$$\sigma = -\frac{3 \cot \theta_0}{s_{44}} \frac{\partial 2\theta_{\psi}}{\partial \sin^2 \psi} = K \cdot M, \tag{13}$$

which indicates that the diffraction angle for each angle $2\theta_{\psi}$ should be linear in $\sin^2 \psi$. In the case of a {112}-oriented CrN film, it was calculated that the CrN-422 diffraction was obtained when the ψ angle was set at 0°, 33.56°, 48.19°, 60.00°, 70.53°, and 80.40°. Due to device limitations, the $\sin^2 \psi$ diagram was drawn using four diffractions below 70°. The stress can be estimated from the slope of the line determined by the least squares method and the elastic compliances of CrN. For crystalline CrN,[19] $s_{11} = 1.85 \times 10^{-3}$ GPa^{-1}, $s_{12} = -0.08 \times 10^{-3}$ GPa^{-1}, and $s_{44} = 11.36 \times 10^{-3}$ GPa^{-1}. When using the CrN-422 diffraction to measure the stress, the stress constant K is calculated to be −2.08 GPa/deg.

The residual stress in the Cr layer was measured by applying the $\sin^2 \psi$ x-ray method[15] to the Cr-310 diffraction at $2\theta = 115.3°$ and using the stress constant $K = -1.35$ GPa/deg calculated by using the Kröner model.[20]

III. EXPERIMENT

A. Preparation of CrN/Cr multilayer films

CrN/Cr multilayer films were deposited by using an arc ion plating system, as shown in Fig. 3. The substrate material was titanium alloy (Ti6Al4V) in the form of $40 \times 29 \times 8$ mm^3 plates. The substrate was polished so that the average surface roughness Ra was 0.1 μm or less and then annealed at 788 °C for 30 min to remove strain. The substrate surface was cleaned for 0.8 min by bombarding with energetic ions accelerated from an arc discharge near a chromium target. After cleaning the substrate, the CrN/Cr multilayer films were deposited. These films were prepared by depositing alternate layers of CrN and Cr. In this study, the total number of layers was six, with an alternating deposition of three Cr films and three CrN films. A cross-sectional SEM image of the CrN/Cr multilayer film is shown in Fig. 4. The total thickness of the multilayer film was about 5.0 μm, and the average thickness of each Cr and CrN layer was about 0.83 μm. The Cr layer was deposited in an argon atmosphere by using an arc current of 70 A and a bias voltage of −150 V. The CrN layers were deposited in a nitrogen atmosphere with the same current and bias voltage. The substrate was then positioned in the chamber so that the substrate surface was orthogonal to the Cr target surface, and the density of droplets on the substrate surface was adjusted by varying the installation height. The height of the center of the Cr target was 170 mm, so the substrate surface was positioned at a greater height.

B. Residual stress measurement conditions

The x-ray equipment for residual stress measurement was based on parallel beam optics. Using a ψ-diffractometer (SmartLab, Rigaku), the diffraction of CrN-422 and Cr-310 was measured to evaluate the residual stress in the CrN layer and Cr layer. CuKα x rays were used for diffraction measurements. The tube voltage and tube current were set to 45 kV and 200 mA, respectively. In the stress measurement of the CrN layer, the x-ray irradiation area was about 0.45×5 mm^2 at $\psi = 0°$.

IV. EXPERIMENTAL RESULTS AND DISCUSSION

A. Surface of CrN/Cr multilayer films

Figure 5 shows micrographs of the surface of CrN/Cr multilayer films, which confirm that the density of droplets on the surface of the multilayer film depends on the height of the substrate. The droplet density was determined by counting the number of droplets in the SEM picture and dividing by the area. Table I shows the relationship between

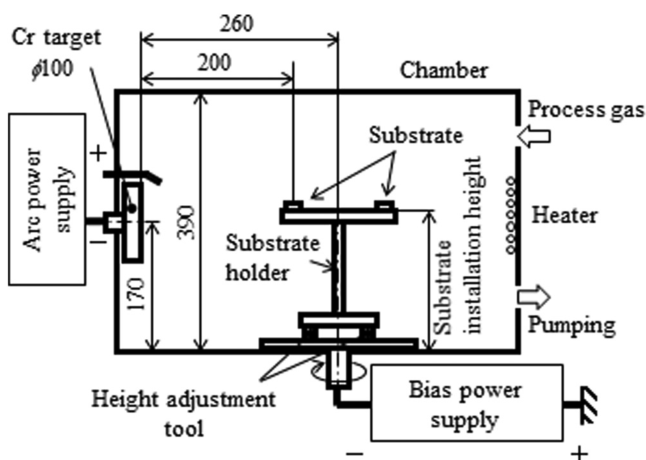

Fig. 3. Film deposition system.

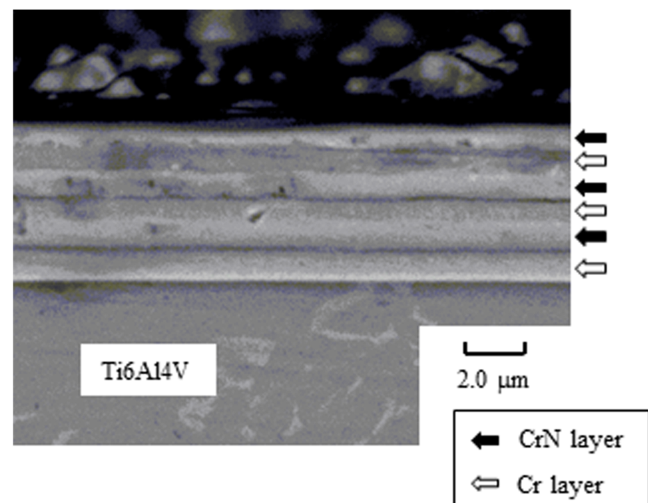

Fig. 4. Cross-sectional SEM image of the CrN/Cr multilayer film.

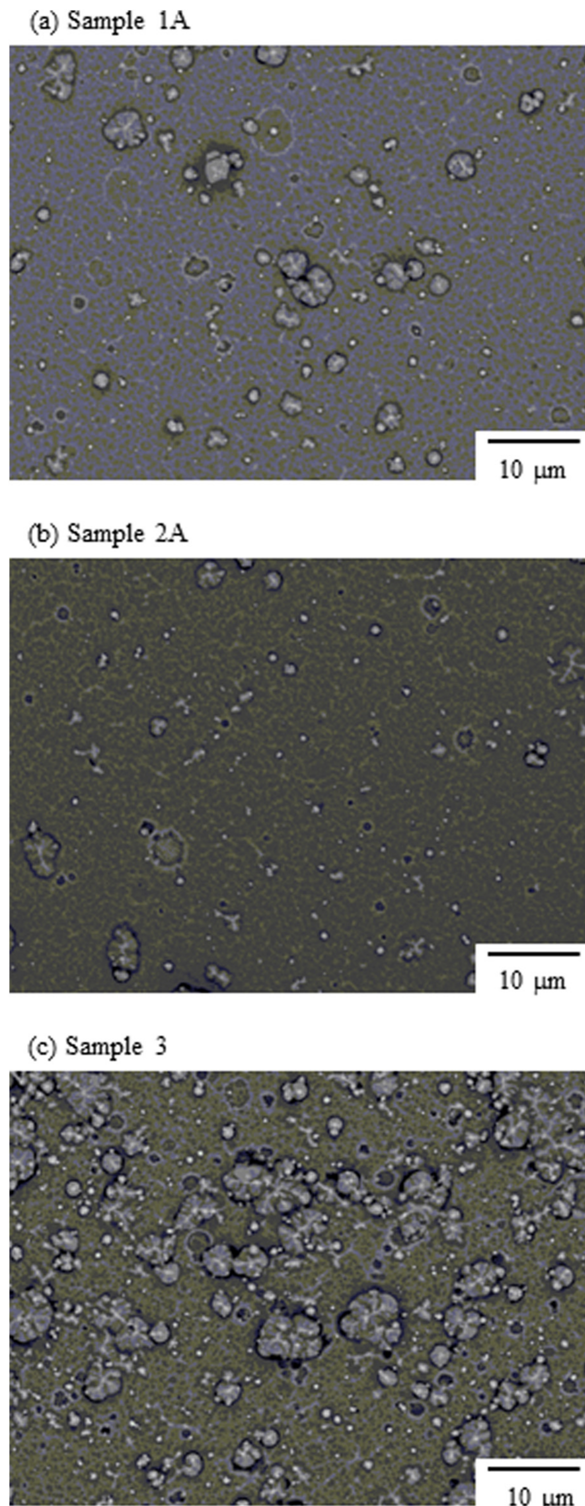

FIG. 5. Micrographs of the surface of CrN/Cr multilayer films. The substrate installation height was (a) 173, (b) 201, and (c) 251 mm.

the substrate installation height and the droplet density on the surface of the multilayer film.

B. Structural evaluation of CrN/Cr multilayer films

Figure 6 shows diffraction patterns from the CrN/Cr multilayer films deposited on the titanium alloy substrate. All

TABLE I. Conditions for CrN/Cr multilayer film deposition.

Sample No.	Substrate installation height (mm)	Number of droplets per unit area (μm^{-2})
1A, 1B	173	6.57×10^{-2}
2A, 2B	201	5.53×10^{-2}
3	251	12.1×10^{-2}

diffractions from the CrN and Cr crystals appear. On the other hand, the diffractions from the Ti6Al4V substrate were hardly confirmed because it was absorbed by the multilayer film deposited on the substrate. The relative intensity of each diffraction from the Cr layer is almost the same as that from Cr powder. However, for the diffraction from the CrN layers, only the CrN-422 diffraction produces a significant intensity. These results indicate that the Cr layer consists of randomly oriented crystals, whereas the CrN layers have a mixed crystalline structure of random orientation and {112} orientation.

C. Residual stress in CrN/Cr multilayer films

Figure 7 show the experimental results for $2\theta_\psi$ as a function of $\sin^2\psi$ for the CrN layers of samples 1A and 2A. The measurement was repeated twice at each angle of $\psi = 0°$, 33.56°, 48.19°, and 60.00°, where the CrN-422 diffraction is significant. The solid (open) circles indicate the measurement result on the $+\psi$ ($-\psi$) side. The results show that the peak $2\theta_\psi$ is nonlinear in $\sin^2\psi$ for all measurements, which is attributed to the triaxial stress state, where the shear component σ_{31} is nonzero or σ_{11} varies with depth in the film. The measurement in the $-\psi$ direction reveals clearly a stress gradient with σ_{11} varying in the depth direction because the ψ split could not be confirmed.[21] In this experiment, a very large compressive residual stress occurs near the substrate-multilayer interface and decreases upon approaching the outer surface of the multilayer. We thus divide the $2\theta_\psi$–$\sin^2\psi$ plot into two regions and use a linear approximation to calculate the residual stress in the CrN layer near the substrate-multilayer interface and near the outer surface

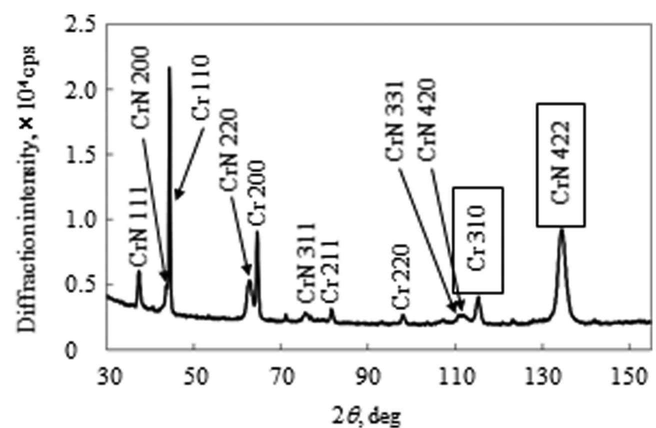

FIG. 6. Diffraction pattern from the CrN/Cr multilayer film deposited on the titanium alloy (sample 1A).

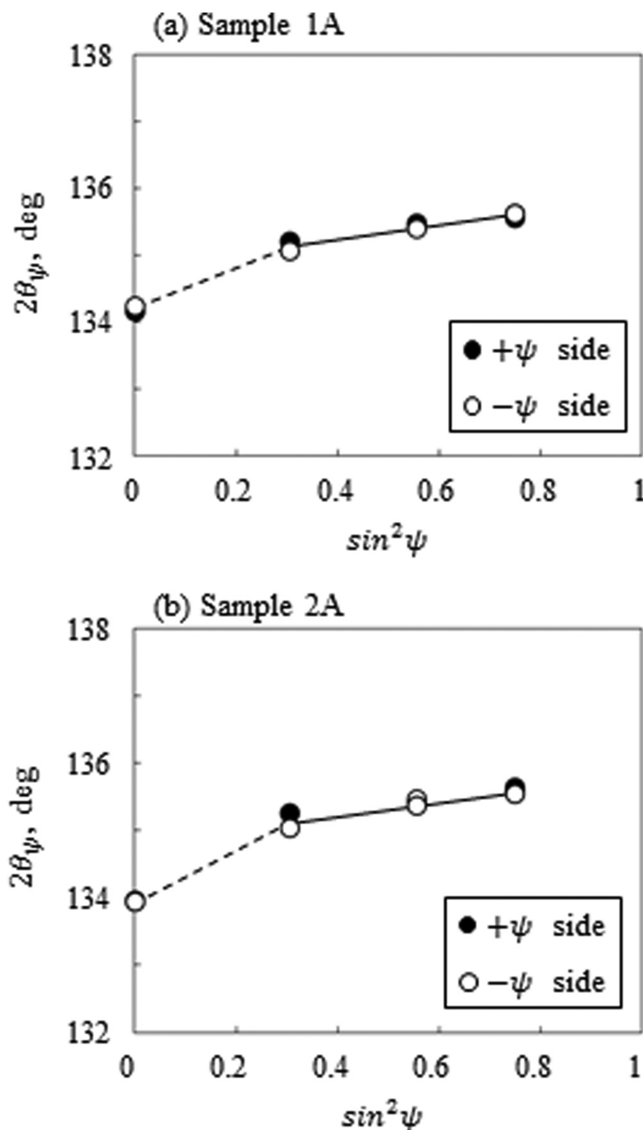

FIG. 7. $2\theta_\psi - \sin^2\psi$ plots for CrN/Cr multilayer films (samples 1A and 2A).

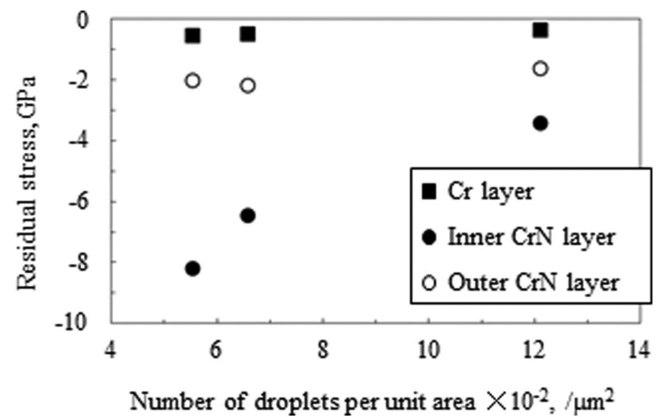

FIG. 8. Residual stress as a function of droplet surface density, showing how droplet density affects residual stress in a CrN/Cr multilayer film.

of the film. The x-ray penetration depth for CrN-422 diffraction in the range of $\sin^2\psi = 0.0$–0.3 was calculated as 2.51–2.09 μm and that in the range of $\sin^2\psi = 0.56$–0.75 was calculated as 1.68–1.26 μm. Therefore, it is considered that the average stress of the outermost CrN layer could be obtained separately from the average stress up to the deeper layer.

Figure 8 shows the residual stress in the Cr and CrN layers as a function of droplet density. The solid squares, solid circles, and open circles indicate the residual stress in the Cr layer, inner CrN layer, and outer CrN layer, respectively. The values of the residual stress in the Cr layer, inner CrN Layer, and outer CrN layer deposited under the condition where the number of droplets per unit area was the smallest (sample 2A) were -0.53 ± 0.02, -8.18 ± 0.16, and -2.01 ± 0.14 GPa, respectively. The same measurement variation was obtained with other samples. A large compressive residual stress occurs in all three layers. The compressive residual stress in both CrN layers is greater than that in the Cr layer. The compressive residual stress is due to ion bombardment.[22,23] Because the CrN layer is harder than the Cr layer, it can withstand greater compressive residual stress.

A large compressive residual stress in the CrN layer forms near the substrate-multilayer interface and decreases significantly with increasing droplet density. In addition, the compressive residual stress in the Cr layer decreases slightly with increasing droplet density. We attribute the reduction in the residual compressive stress near the surface of the outer CrN layer to be caused by the surface roughness due to the presence of droplets. The droplets consist of metallic Cr melted and ejected from the target during film deposition. Since metallic Cr metal is softer than CrN, we suggest that the droplets mixed into the CrN layer are plastically deformed due to the large residual compressive stress. As a result, it is considered that the residual compressive stress in the CrN layer decreases with increasing droplet density.

V. CONCLUSION

We developed and verified an x-ray analysis method to measure the residual stress in the {112}-oriented film and use it to measure the residual stress in CrN/Cr multilayer films deposited on titanium alloy substrates. In addition, we investigate how the density of Cr droplets on the surface of the film affects the residual stress in these multilayer films. The results lead to the following conclusions:

(1) The residual stress of the {112}-oriented film may be measured by measuring the CrN-422 diffraction peak at four different angles of ψ.
(2) Residual compressive stress develops in both the Cr layer and the CrN layer of the CrN/Cr multilayer film, and the compressive stress in the harder CrN layer is greater than in the softer Cr layer.
(3) In the CrN layers, a stress gradient appears as a result of relaxation of residual compressive stress at the surface of the outer CrN layer. On the contrary, no stress gradient appears in the Cr layer.
(4) The large residual compressive stress that forms in the CrN layer near the substrate-multilayer interface decreases significantly with increasing droplet density.

ACKNOWLEDGMENTS

The author is grateful to the contributions of all the students, including Satoshi Nakai and Kazushi Nishimura, who were involved in sample preparation. The authors would like to acknowledge Enago (www.enago.jp) for the English language review.

[1]A. Kondo, T. Oogami, K. Sato, and Y. Tanaka, Surf. Coat. Technol. **177–178**, 238 (2004).
[2]A. Lousa, J. Romero, E. Martı´nez, J. Esteve, F. Montalà, and L. Carreras, Surf. Coat. Technol. **146–147**, 268 (2001).
[3]E. Broszeit, C. Friedrich, and G. Berg, Surf. Coat. Technol. **115**, 9 (1999).
[4]C. Öner, H. Hazar, and M. Nursoy, Mater. Des. **30**, 914 (2009).
[5]P. Wieciński, J. Smolik, H. Garbacz, and K. J. Kurzydłowski, Surf. Coat. Technol. **240**, 23 (2014).
[6]D. Yonekura, J. Fujita, and K. Miki, Surf. Coat. Technol. **275**, 232 (2015).
[7]T. Polcar and A. Cavaleiro, Mater. Chem. Phys. **129**, 195 (2011).
[8]F. Cai, S.-H. Zhang, J.-L. Li, Z. Chen, M.-X. Li, and L. Wang, Appl. Surf. Sci. **258**, 1819 (2011).
[9]Y.-P. Feng, L. Zhang, R.-X. Ke, Q.-L. Wan, Z. Wang, and Z.-H. Lu, Int. J. Refract. Metals Hard Mater. **43**, 241 (2014).
[10]K. Alexander, P. Sergej, and S. Volodymyr, Appl. Surf. Sci. **477**, 2 (2019).
[11]G. Abadias *et al.*, J. Vac. Sci. Technol. A **36**, 020801 (2018).
[12]P. Wieciński, J. Smolik, H. Garbacz, and K. J. Kurzydlowski, Thin Solid Films **519**, 4069 (2011).
[13]P. Wieciński, J. Smolik, H. Garbacz, and K. J. Kurzydłowski, Vacuum **107**, 277 (2014).
[14]P. Wieciński, J. Smolik, H. Garbacz, and K. J. Kurzydłowski, Surf. Coat. Technol. **309**, 709 (2017).
[15]The Society of Materials Science, Japan, JSMS-SD-10-05, 2005.
[16]K. Tanaka, K. Ishihara, and K. Inoue, J. Soc. Mater. Sci. Jpn. **45**, 945 (1996) (in Japanese).
[17]S. Ejiri, T. Sasaki, and Y. Hirose, J. Soc. Mater. Sci. Jpn. **46**, 750 (1997) (in Japanese).
[18]J. F. Nye, *Physical Properties of Crystals* (Oxford University, New York, 1957), p. 134.
[19]M. Birkholz, *Thin Film Analysis by X-ray Scattering* (Wiley-VCH, Weinheim, 2005), p. 259.
[20]E. Kröner, Z. Phys. **151**, 504 (1958).
[21]I. C. Noyan, Metall. Trans. A **14**, 249 (1983).
[22]C. A. Davis, Thin Solid Films **226**, 30 (1993).
[23]P. J. Martin, A. Bendavid, T. J. Kinder, and L. Wielunski, Surf. Coat. Technol. **86–87**, 271 (1996).